*Eleventh International Conference on CFD in the Minerals and Process Industries*
*CSIRO, Melbourne, Australia*
*7-9 December 2015*

# DIRECT NUMERICAL SIMULATIONS OF FLUID DRAG FORCES OF NON-SPHERICAL PARTICLE

**Sathish K. P. SANJEEVI**[1*], **Johan T. PADDING**[1], **J. A. M. KUIPERS**[1]
[1]Department of Chemical Engineering and Chemistry, Eindhoven University of Technology,
P.O. Box 513, 5600MB Eindhoven, The Netherlands
[*] E-mail: s.k.pacha.sanjeevi@tue.nl

## ABSTRACT

In the modelling of particle fluidization, it is traditionally assumed that the particles are spherical in shape, as this greatly simplifies the representation of gas-solid drag and particle collisions. However, several industrial processes involve particles which are highly non-spherical in nature. For example, bio-mass gasification process involves milled bio-mass, which could be approximated as sphero-cylindrical in shape. This work involves direct numerical simulation of a single non-spherical particle. The aim of this study is to characterize the drag coefficient based on the Reynolds number with particle orientation. The simulations are performed using the lattice Boltzmann method. The results from these simulations can be later extended to multi-particle assemblies, which can be used to derive drag, lift and torque closures for coarse-grained discrete particle simulations.

**Keywords:** LBM, DNS, Non-spherical particle.

## NOMENCLATURE

| | |
|---|---|
| $\varepsilon$ | Solids volume fraction |
| $\mu$ | Dynamic viscosity of the fluid |
| $\nu$ | Kinematic viscosity |
| $\omega_i$ | Proportionality constant |
| $\Phi$ | Sphericity |
| $\phi$ | Incident angle |
| $\rho$ | Macroscopic density |
| $\tau$ | Relaxation time |
| $C_D$ | Drag coefficient |
| $c_s$ | Lattice speed of sound |
| $D_p$ | Equivalent particle diameter |
| $d_p$ | Diameter of sphere |
| $F$ | Dimensionless force |
| $f_i$ | Distribution function |
| $F_{f\rightarrow s}$ | Force exerted by fluid on particle |
| $f_i^{(eq)}$ | Equilibrium distribution function |
| $h$ | Lattice/grid length |
| $Re$ | Reynolds number |
| $U_0$ | Superficial velocity |
| $U_\infty$ | Relative fluid velocity with respect to particle |

## INTRODUCTION

Practical applications of gas-solid fluidized systems often involve particles which are non-spherical, of either regular or irregular shapes. Therefore, exclusive drag, lift and torque closures must be developed, which are particle shape specific. Several drag closures have been proposed in the past based on experiments [Ergun (1952); Wen and Yu (1966)] and simulations for mono, bi- and poly-disperse spheres [Beetstra *et al.* (2007); Van der Hoef *et al.* (2005); Tenneti *et al.* (2011); Yin and Sundaresan (2008, 2009)] as a function of Reynolds number $Re$ and solids volume fraction $\phi$. One of the earliest and widely popular drag closures is from Ergun (1952) for randomly packed beds. Hill *et al.* (2001) in their work use lattice Boltzmann simulations to investigate the drag force for small to moderate Reynolds number flows with ordered and random array of spheres. The proposed correlation covers the Reynolds number range of 30-100 and volume fractions in the range 0.1-0.64. Van der Hoef *et al.* (2005) and Beetstra *et al.* (2007) proposed drag laws for mono- and bi-disperse arrays of spheres for low and intermediate Reynolds numbers respectively. Recently, Yin and Sundaresan (2008) proposed a drag law for flows at low Reynolds number with bi-disperse spheres with $\phi_1/\phi_2$ from 1 : 1 to 1 : 7 and particle volume fraction from 0.1 to 0.4. Tenneti *et al.* (2011) propose a drag law for mono-disperse spheres for Reynolds number ranging $0.01 \leq Re \leq 300$ and solid volume fraction $0.1 \leq \phi \leq 0.5$ using particle resolved direct numerical simulations.

The afore-mentioned drag laws are for assemblies of spherical particles. To the authors' knowledge, no drag closures for assemblies of non-spherical particles have been proposed yet, let alone lift and torque closures. However, there are several works recently reported for non-spherical particle fluidization simulations using the discrete particle method (DPM) [Zhou *et al.* (2009, 2011); Zhong *et al.* (2009); Hilton *et al.* (2010); Ren *et al.* (2012, 2013); Oschmann *et al.* (2014)]. They use either empirical drag cor-

| Models | Equations | Particle orienta-tion |
|---|---|---|
| Haider and Levenspiel (1989) | $C_D = \frac{24}{Re}(1+A.Re^B) + \frac{C}{1+D/Re}$<br>$A,B,C,$ and $D$ are functions of particle sphericity $\Phi$ | ✗ |
| Tran-Cong *et al.* (2004) | $C_D = \frac{24}{Re}\frac{d_A}{d_n}\left[1+\frac{0.15}{\sqrt{c}}\left(\frac{d_A}{d_n}Re\right)^{0.687}\right] + \frac{0.42(d_A/d_n)^2}{\sqrt{c}\left[1+4.25\times10^4\left(\frac{d_A}{d_n}Re\right)^{-1.16}\right]}$<br>$d_A$ and $d_n$ are surface-equivalent sphere and nominal diameter<br>$c$ is particle circularity | ✓ |
| Hölzer and Sommerfeld (2008) | $C_D = \frac{8}{Re}\frac{1}{\sqrt{\Phi_\parallel}} + \frac{16}{Re}\frac{1}{\sqrt{\Phi}} + \frac{3}{\sqrt{Re}}\frac{1}{\Phi^{3/4}} + 0.4210^{0.4(-\log\Phi)^{0.2}}\frac{1}{\Phi_\perp}$<br>$\Phi$, $\Phi_\parallel$, and $\Phi_\perp$ are regular, lengthwise and crosswise sphericity | ✓ |
| Mandø and Rosendahl (2010) | $C_D(\phi) = C_{D,\phi=0^0} + (C_{D,\phi=90^0} - C_{D,\phi=0^0})\sin^3(\phi)$ | ✓ |

Table 1: Summary of different drag models for non-spherical particles.

relations (parametrized with aspect ratio and other parameters) proposed for different non-spherical particles or use a multi-sphere approach to approximate complex particle shapes. Therefore, all these simulations do not consider the true geometry of the particles and therefore the reported results may not truly represent actual conditions.

Table 1 summarizes the different drag models available for non-spherical particles. One of the earliest empirical correlations is the one from Haider and Levenspiel (1989), which however does not include particle orientation information and therefore effectively is not suitable for particles of arbitrary shape. The correlation of Tran-Cong *et al.* (2004), however includes orientation information, but the non-spherical particles themselves are created by gluing multiple spheres together to get the desired particle shape, which introduces surface roughness. Hölzer and Sommerfeld (2008) proposed a correlation, which includes two different projected areas to represent particle orientation - both lengthwise and crosswise. It is created from a large set of experimental data reported in literature and also extensive numerical simulations. The equation has been tested with different particle shapes such as ellipsoids, cuboids and cylinders. The mean deviation is found to be 14.4% and max. deviation of 29% reported for cuboids and cylinders, compared with experimental results reported in literature. Since this correlation involves extensive data, we compare our simulation results with the same and Zastawny *et al.* (2012) involving the DNS.

In this work, we perform direct numerical simulations using lattice Boltzmann method (LBM) to simulate flow around a single non-spherical particle. We will show that the LBM predictions are in good agreement with results obtained from more traditional direct numerical simulation methods. This opens the way to develop closures for lift, drag and torque in multi-particle assemblies.

## LATTICE BOLTZMANN METHOD

The lattice Boltzmann equation is based on discretizing the BGK equation. Ignoring volume forces, it is given by

$$f_i(\vec{x}+\vec{c}_i\Delta t, t+\Delta t) = f_i(\vec{x},t) + \frac{1}{\tau}(f_i^{(eq)}(\vec{x},t) - f_i(\vec{x},t)), \quad (1)$$

where $f_i^{(eq)}(\vec{x},t)$ is the equilibrium distribution function and $\tau$ is the relaxation time. The LBM simulations are performed in lattice units and time is incremented using unit timestep $\Delta t = 1$:

$$f_i(\vec{x}+\vec{c}_i, t+1) = f_i(\vec{x},t) + \frac{1}{\tau}(f_i^{(eq)}(\vec{x},t) - f_i(\vec{x},t)). \quad (2)$$

The above equation is solved in two separate steps at each timestep:

$$\textbf{Collision :}\ f_i'(\vec{x},t+1) = f_i(\vec{x},t) + \frac{1}{\tau}(f_i^{(eq)}(\vec{x},t) - f_i(\vec{x},t)), \quad (3)$$

$$\textbf{Streaming :}\ f_i(\vec{x}+\vec{c}_i,t+1) = f_i'(\vec{x},t+1). \quad (4)$$

The lattice model used in our simulations is D3Q19. The equilibrium distribution function $f_i^{(eq)}(\vec{x},t)$ derived from the Maxwell-Boltzmann velocity distribution equation for isothermal condition is given by

$$f_i^{(eq)} = \rho\omega_i\left(1+\frac{\vec{c}_i.\vec{u}}{c_s^2} - \frac{\vec{u}.\vec{u}}{2c_s^2} + \frac{(\vec{u}.\vec{c}_i)^2}{2c_s^4}\right) . \quad (5)$$

where $\rho$ is the macroscopic density, $\vec{u}$ is the macroscopic velocity, $c_s$ is the speed of sound in lattice units $c_s = \frac{1}{\sqrt{3}}\frac{\Delta x}{\Delta t}$ and $\omega_i$ is the proportionality constant. The macroscopic variables such as flow density $\rho$ and velocity $\vec{u}$ are calculated as,

$$\rho = \sum_i f_i \tag{6}$$

$$\vec{u} = \frac{1}{\rho} \sum_i \vec{c}_i f_i \tag{7}$$

The relaxation time $\tau$ relates to the lattice viscosity $\nu$ by the following relation,

$$\nu = c_s^2 \left( \tau - \frac{1}{2} \right) \tag{8}$$

## VALIDATION TESTCASES

### Stokes flow for a simple cubic configuration

Prior to the actual non-spherical particles simulation, a validation simulation with spherical particles is being performed and compared with literature [Kriebitzsch (2011)]. In the actual simulation, a single spherical particle in simple cubic configuration with periodic boundaries is simulated at various volume fractions at Stokes flow ($Re \approx 0$). The fluid is subjected to a gravitational field and the particle is fixed in space. The resulting parameter of interest is non-dimensionalized drag force for a single particle $F$ with respect to the solid volume fraction defined by,

$$F = \frac{F_{f \to s}}{3\pi\mu U_0 d_p} \tag{9}$$

where $F_{f \to s}$ is the force exerted by fluid on the particle, $\mu$ is the dynamic viscosity of the fluid, $U_0$ is the superficial velocity and $d_p$ is the particle diameter.

*LBM simulation parameters*

Table 2 contains the parameters used in the simulations in lattice units. These parameters were maintained constant throughout all simulations. Table 3 contains parameters which were modified for different simulations and corresponding dimensionless drag force $F$ measured. The dimensionless drag force $F$ as function of solids volume fraction is given in Fig. 1. It can be observed that the results from LBM agree well with literature results obtained from DNS simulations [Kriebitzsch (2011)].

| Parameter | Value |
|---|---|
| Domain size | $64 \times 64 \times 64$ |
| Gravitational field for fluid forcing | $2 \times 10^{-5}$ |
| Number of iterations | 15000 |
| Relaxation time | 1.0 |
| Kinematic viscosity | $1/6$ |

Table 2: Fixed parameters for all LBM simulations in lattice units.

| Sphere radius | Volume fraction | $F$ | $U_0$ |
|---|---|---|---|
| 19 | 0.11 | 3.975 | 0.0221 |
| 23 | 0.194 | 6.704 | 0.0108 |
| 28 | 0.351 | 17.530 | 0.0034 |
| 31 | 0.476 | 32.908 | 0.0016 |
| 31.5 | 0.499 | 37.286 | 0.0014 |

Table 3: Sphere radius, volume fraction and the respective dimensionless drag force $F$ and superficial velocity $U_0$ measured.

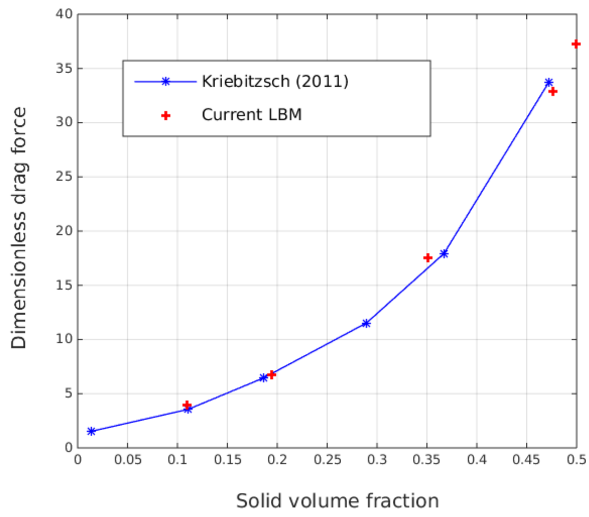


Figure 1: Dimensionless drag force $F$ as a function of solids volume fraction for Stokes flow.

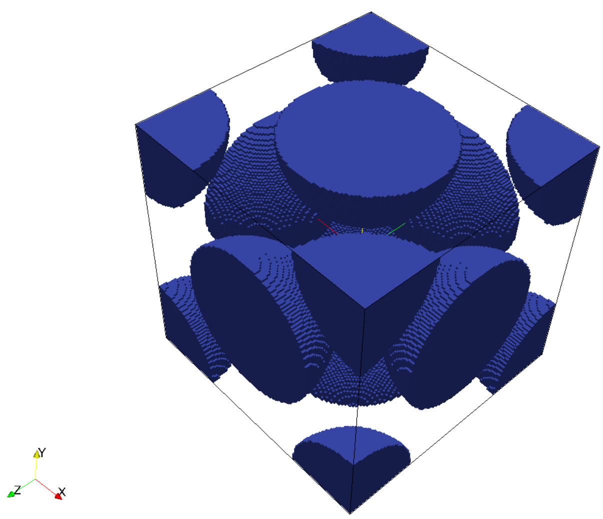


Figure 2: Face centered cubic (FCC) configuration.

### Resolution free force for a FCC configuration

As another validation test case, flow around spheres in a face-centered-cubic (FCC) configuration (see Fig.2) is simulated at moderate Reynolds number $Re = 100$ and solids volume fraction, $\varepsilon = 0.4$. The simulation domain is cubic in shape with side lengths ranging from 40 upto 256 and corresponding sphere radius of 11.517 upto 73.713 in lattice units respectively. The desired $Re$ is achieved through the combination of fluid gravitational field and viscosity. The lowest relaxation parameter used is 0.5025 and the corresponding kinematic viscosity is 0.0008333. The results are then compared with Tang *et al.* (2014). The "resolution-free" drag force $F_\infty$ is computed by fitting the simulation data obtained at different resolutions $(d_p/h)$ to the form, $F = F_\infty + C \cdot (d_p/h)^{-2}$, where $C$ is a constant and is plotted in Fig. 3. Present LBM simulations provide the equation to be of form,

$$F = 36.254 + 14180 \cdot (d_p/h)^{-2} \qquad (10)$$

compared to the DNS simulations of Tang *et al.*,

$$F = 35.906 + 7821.05 \cdot (d_p/h)^{-2} \qquad (11)$$

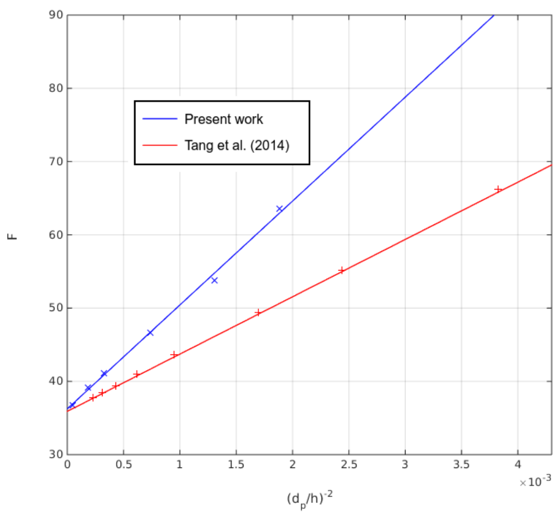


Figure 3: The dimensionless force $F$ obtained from simulations at different grid resolutions, as function of $(d_p/h)^{-2}$. The present work takes the form $F = 36.254 + 14180 \cdot (d_p/h)^{-2}$ compared to Tang *et al.* with $F = 35.906 + 7821.05 \cdot (d_p/h)^{-2}$.

The present "resolution-free" force of $F_\infty = 36.254$ is in close agreement with the literature and within less than 1% difference. The difference in slopes is due to different numerical methods - the present with LBM and the literature with Navier-Stokes based immersed boundary method DNS. The reason specifically LBM under-performs is due to first order explicit discretization of the Boltzmann equation, compared to second order discretization of momentum equations of NS based DNS. More details on the NS DNS numerical scheme can be found in Tang *et al.* (2014).

## RESULTS

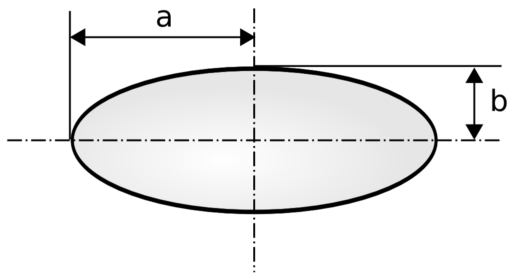


Figure 4: The "Ellipsoid 1" from Zastawny *et al.* (2012) with $a/b = 5/2$ (and $b = c$, implying prolate ellipsoid) with sphericity $\Phi = 0.886$.

The recent publication from Zastawny *et al.* (2012) contains detailed flow simulation results of prolate, oblate ellipsoid and fibre at different angles of attack. The particle of our investigation is a prolate ellipsoid referenced "Ellipsoid 1" in Zastawny *et al.* (2012) with radii ratio $a/b = 5/2$ and $b = c$ as in Fig. 4. The sphericity $\Phi$ of a non-spherical particle is given by the ratio of surface area of volume equivalent sphere as non-spherical particle with respect to surface area of the non-spherical particle itself. The particle under investigation has sphericity, $\Phi = 0.886$. The LBM flow solver used is highly scalable, parallelized with MPI and has been tested with linear scaling up to 262,144 cores as reported in Harting *et al.* (2012).

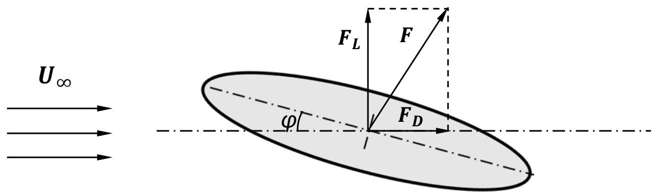


Figure 5: Forces acting on an inclined non-spherical particle.

| Parameter | Value |
|---|---|
| Domain size | $192 \times 192 \times 336$ |
| Equivalent particle diameter $D_p$ | 20 |
| Number of time steps/iterations | $1.5 \times 10^5$ |

Table 4: Variables used in LBM simulations in lattice units.

The Reynolds number is given by $Re = \frac{U_\infty D_p}{\nu}$, where $D_p$ represents the equivalent particle diameter of the non-spherical particle based on a sphere with equivalent volume. The range of Reynolds numbers simulated is $0 < Re \leq 100$. For a sphere, the flow is still laminar for the range of $Re$ covered here and therefore, we assume the grid resolution is sufficient for the detailed DNS of the non-spherical particle. The simulation domain is of size

$10D_p \times 10D_p \times 17.5D_p$ for all $Re$. In the actual simulations, the particle is moved with a constant force in the quiescent fluid. The desired $Re$ is achieved by varying forcing and lattice kinematic viscosity $\nu$. As the fluid domain is periodic, the particle forcing continuously adds momentum to the fluid. Therefore, the force is balanced by applying a counteracting force equally distributed in all the fluid cells. The maximum number of processors used in the simulations is 3072. The relevant parameters are summarized in table 4. As mentioned in Fig. 5, a non-spherical particle inclined to the incident flow experiences both lift and drag force. The incident angle investigated here is $\phi = 0^\circ, 90^\circ$, where the particle experiences only drag because of symmetry.

## Drag force

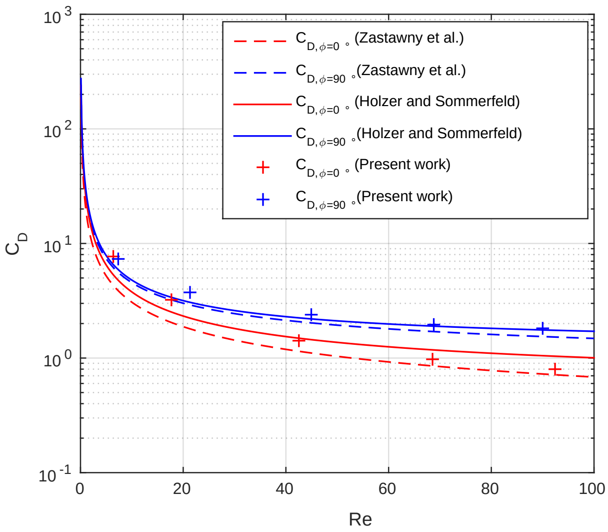


Figure 6: Drag coefficient $C_D$ of the non-spherical particle with respect to Reynolds number $Re$.

It can be observed from Fig. 6 that the simulated results follow the trends of both Zastawny *et al.* (2012) and Hölzer and Sommerfeld (2008). For incident angle $\phi = 0^\circ$ at $Re \geq 40$, the measured $C_D$ lies within the reported range in the literature. However at $Re < 40$, it can be observed that the measured drag from simulations is comparatively larger than correlations from literature. Particularly the deviation is higher in case of $\phi = 0^\circ$ (upto 20% at low $Re$), where the flow incident cross section area is smaller and hence represented by a lower number of lattice cells. This introduces stronger approximation of the boundary as a staircase order leading to higher measured drag at low $Re$. In case of $\phi = 90^\circ$, the agreement is better for all $Re$ and close to reported results in literature, as the effective cross section is represented by a larger number of lattice cells.

## CONCLUSION

In this work, we performed direct numerical simulations of flow around a single non-spherical particle at different orientation using the lattice Boltzmann method. It is observed that there is good agreement between simulated and literature results for a single particle. This opens the way to simulate multi-particle assemblies, generating closures for lift, drag and torque coefficients.

## ACKNOWLEDGEMENT


The authors thank the European Research Council for its financial support under its Consolidator Grant scheme, Contract no. 615906 (NonSphereFlow).


## REFERENCES


BEETSTRA, R. *et al.* (2007). “Drag force of intermediate Reynolds number flow past mono-and bidisperse arrays of spheres”. *AIChE Journal*, **53(2)**, 489–501.

ERGUN, S. (1952). “Fluid flow through packed columns”. *Chem. Eng. Prog.*, **48(2)**, 89–94.

HAIDER, A. and LEVENSPIEL, O. (1989). “Drag coefficient and terminal velocity of spherical and nonspherical particles”. *Powder technology*, **58(1)**, 63–70.

HARTING, J. *et al.* (2012). “Coupled lattice Boltzmann and molecular dynamics simulations on massively parallel computers”. *Proceedings: 25 years HLRZ/NIC, 7-8 February 2012, Jülich, Germany. 2012*, **45**, 243.

HILL, R.J. *et al.* (2001). “Moderate Reynolds number flows in ordered and random arrays of spheres”. *Journal of Fluid Mechanics*, **448**, 243–278.

HILTON, J. *et al.* (2010). “Dynamics of gas-solid fluidised beds with non-spherical particle geometry”. *Chemical Engineering Science*, **65(5)**, 1584 – 1596.

HÖLZER, A. and SOMMERFELD, M. (2008). “New simple correlation formula for the drag coefficient of non-spherical particles”. *Powder Technology*, **184(3)**, 361–365.

KRIEBITZSCH, S. (2011). *Direct numerical simulation of dense gas-solids flows*. Ph.D. thesis, Technische Universiteit Eindhoven.

MANDØ, M. and ROSENDAHL, L. (2010). “On the motion of non-spherical particles at high Reynolds number”. *Powder Technology*, **202(1)**, 1–13.

OSCHMANN, T. *et al.* (2014). “Numerical investigation of mixing and orientation of non-spherical particles in a model type fluidized bed ”. *Powder Technology*, **258(0)**, 304 – 323.

REN, B. *et al.* (2012). “CFD-DEM simulation of spouting of corn-shaped particles”. *Particuology*, **10(5)**, 562 – 572.

REN, B. *et al.* (2013). “Numerical simulation on the mixing behavior of corn-shaped particles in a spouted bed”. *Powder Technology*, **234(0)**, 58 – 66.

TANG, Y. *et al.* (2014). “A methodology for highly accurate results of direct numerical simulations: Drag force in dense gas–solid flows at intermediate Reynolds number”. *International journal of multiphase flow*, **62**, 73–86.

TENNETI, S. *et al.* (2011). “Drag law for monodisperse gas-solid systems using particle-resolved direct numerical simulation of flow past fixed assemblies of spheres”. *International journal of multiphase flow*, **37(9)**, 1072–1092.

TRAN-CONG, S. *et al.* (2004). “Drag coefficients of irregularly shaped particles". *Powder Technology*, **139(1)**, 21–32.

VAN DER HOEF, M. *et al.* (2005). "Lattice Boltzmann simulations of low Reynolds number flow past mono-and bidisperse arrays of spheres: results for the permeability and drag force". *Journal of fluid mechanics*, **528**, 233–254.

WEN, C.Y. and YU, Y.H. (1966). "Mechanics of fluidization". *Chemical Engineering Progress, Symposium Series*, **62(1)**, 100–111.

YIN, X. and SUNDARESAN, S. (2008). "Drag law for bidisperse gas-solid suspensions containing equally sized spheres". *Industrial & Engineering Chemistry Research*, **48(1)**, 227–241.

YIN, X. and SUNDARESAN, S. (2009). "Fluid-particle drag in low-Reynolds-number polydisperse gas–solid suspensions". *AIChE journal*, **55(6)**, 1352–1368.

ZASTAWNY, M. *et al.* (2012). "Derivation of drag and lift force and torque coefficients for non-spherical particles in flows". *International Journal of Multiphase Flow*, **39**, 227–239.

ZHONG, W. *et al.* (2009). "Discrete Element Method Simulation of Cylinder-Shaped Particle Flow in a Gas-Solid Fluidized Bed". *Chemical engineering & technology*, **32(3)**, 386–391.

ZHOU, Z. *et al.* (2009). "CFD-DEM simulation of gas fluidization of ellipsoidal particles". *Proceedings of the Seventh International Conference on CFD in the Minerals and Process Industries, CSIRO, Melbourne, Australia.*

ZHOU, Z. *et al.* (2011). "Discrete particle simulation of gas fluidization of ellipsoidal particles". *Chemical Engineering Science*, **66(23)**, 6128 – 6145.

 